Dalton Transactions

Captivation with Encapsulation: A dozen years of exploring uranyl peroxide capsules

Journal:	*Dalton Transactions*
Manuscript ID	DT-FRO-11-2017-004245.R1
Article Type:	Frontier
Date Submitted by the Author:	11-Mar-2018
Complete List of Authors:	Burns, Peter; University of Notre Dame, Department of Civil Engineering Nyman, May; Oregon State University, Chemistry

Captivation with Encapsulation: A dozen years of exploring uranyl peroxide capsules

Peter C. Burns

Department of Civil and Environmental Engineering and Earth Sciences, University of Notre Dame, Notre Dame, IN 46556, USA
Department of Chemistry and Biochemistry, University of Notre Dame, Notre Dame, IN 46556, USA

May Nyman

Department of Chemistry, Oregon State University; Corvallis, OR 97331, USA

Abstract

Uranyl peroxide clusters containing from 16 to 124 uranyl ions self-assemble in aqueous solution and exhibit tremendous topological complexity. Most of these clusters are cages, with the inside and outside surfaces passivated by oxygen atoms that are triply bonded to U(VI) cations (yl oxygen). It has become increasing apparent that the counter cations associated with these anionic cage clusters impact their assembly, topologies, and behavior in solution, including aggregation and aqueous solubility. Here we review the chemical compositions and topologies of uranyl peroxide clusters. We focus attention on the role of counter cations in cluster assembly, the properties of clusters in solution including supramolecular assembly, thermodynamic studies, and endohedral encapsulation. We also review the most useful solution characterization techniques of the counter cations and counter cation-capsule interactions. Potential applications in nuclear fuel cycles are discussed, including exerting nanoscale control of actinides to revolutionize separations technologies and provide novel pathways to nuclear materials including fuels, and an improved understanding of the transport of uranium in various systems. Finally, we elucidate some future directions.

Introduction

Metal oxide clusters are applied in life science,[1-5] materials science,[6-8] energy[9, 10] and the environment.[11, 12] They provide a unique perspective to understand structure-size-property relations.[13, 14] They serve as models for the metal oxide-water interface that is important in both geochemical reactions[15] and chemical synthesis.[16] Transition metal polyoxometalates (POMs) are anionic metal-oxo clusters that contain high-valence group V/VI cations.[13, 14] These are unique amongst the transition metals because the terminal multiply-bonded oxo ligand passivates the outside of the cluster, preventing aggregation and precipitation of the compositionally similar metal oxide material.

While the high-valent actinides (i.e. U^{VI}, Np^{V}) likewise speciate as 'yl' complexes with multiply-bound oxo ligands, it is only during the last decade that a major family of actinide-based POMs

has emerged,[17, 18] and these have several commonalities with the transition metal POMs.[17] The actinide peroxide POMs are predominantly uranyl peroxide cage clusters that self-assemble in water at room temperature.[17, 18] Small-angle X-ray scattering (SAXS) studies have established that uranyl peroxide cages form and are stable in aqueous solutions, and X-ray diffraction studies of crystals formed from such solutions revealed their atomic-scale detail. The initial report in 2005 described three clusters, U_{24}, U_{28} and U_{32} (Fig. 1, U_n indicates a cluster containing *n* uranyl polyhedra, cluster formulae are in Table 1).[19]

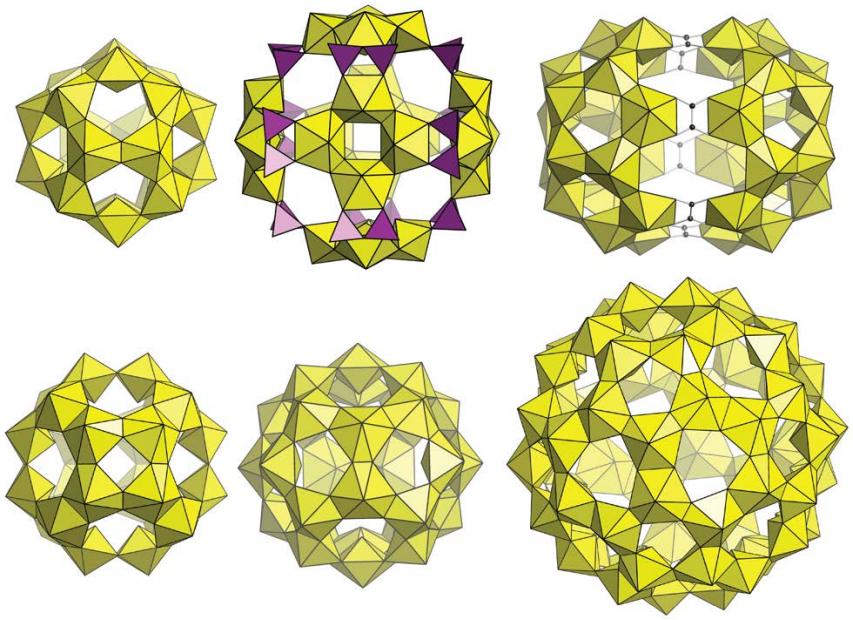

Figure 1. Examples of uranyl peroxide cage clusters. Top, from left: U_{20}, $U_{24}Pp_{12}$, $U_{36}Ox_6$. Bottom, from left: U_{24}, U_{28}, U_{60}. Models are drawn at the same scale. Note that U_{20} contains only topological pentagons, U_{24} contains topological squares and hexagons, and U_{60} contains topological pentagons and hexagons. U_{20} and U_{60} have fullerene topologies. Uranyl polyhedra are shown in yellow, phosphate tetrahedra in purple, and carbon atoms in black.

Hexavalent uranium in water forms linear $(UO_2)^{2+}$ uranyl ions that dominate U(VI) solid state and aqueous chemistry, as well as mineralogy. Triple U-O_{yl} bonds (1.8 Å) render the O_{yl} atoms largely chemically unreactive towards further strong bond formation, and stabilize uranyl peroxide cages at both the outer and inner surfaces,[17] giving rise to their capsule topologies. Transition metal POMs can likewise exhibit capsule topologies, and these are limited to Mo and V, whose small ionic radii favor square pyramidal coordination geometry, and the base of the pyramids define the inside of the capsule. These transition metal POM capsules usually contain mixed valency of W^{VI}, $Mo^{V/VI}$ and $V^{IV/V}$.[20-23]

The anionic uranyl peroxide cages are balanced by simple cations that are most commonly alkalis.[18] Assembly of the cage occurs in as little as a few minutes,[24] although formation can take several days or more in some cases.[25,26] We have growing evidence that the counter

cations plays a significant role in the rate of capsule formation (discussed below). Here we summarize the current literature concerning uranyl peroxide clusters. We first describe structures of different classes of clusters based on their bridging ligands and monomer building blocks, and then describe the role and behavior of the counter cations in directing self-assembly, dissolution and precipitation, supramolecular-assembly and solvent extraction. We describe solution characterization techniques that have been particularly useful and identify some possible applications of uranyl peroxide cages within the nuclear fuel cycle. We also discuss advances in heterometallic capsules, where the heterometals have been incorporated in both the capsule shell and encapsulated to form endohedral topologies. Finally, we identify several outstanding directions for further research.

Table 1. Notations and cluster compositions for uranyl peroxide clusters discussed in the text.

Symbol	Cage Composition
U_{16}	$[(UO_2)_{16}(O_2)_{24}(OH)_8]^{24-}$
$U_{16}L_8$	$[(UO_2)_{16}(O_2)_{16}[(PO_3)_2C(OH)CH_3]_8]^{32-}$
$U_{16}L_8P_4$	$[(UO_2)_{16}(O_2)_8(OH)_8[(PO_3)_2C(OH)CH_3]_8(PO_4)_4]^{28-}$
$U_{18}Pp_2PCP_6$	$[(UO_2)_{18}(O_2)_{18}(OH)_2(CH_2P_2O_6)_6(P_2O_7)_2]^{34-}$
$U_{18}W_2P_{12}$	$[(UO_2)_{18}(O_2)_{15}(W_2O_6(OH)_3)(H_2PO_4)(H_2O)_6]^{9-}$
U_{20}	$[(UO_2)_{20}(O_2)_{30}]^{20-}$
$U_{20}Pp_{6b}$	$[(UO_2)_{20}(O_2)_{24}(P_2O_7)_6]^{32-}$
$U_{20}Pp_{6a}$	$[(UO_2)_{20}(O_2)_{24}(P_2O_7)_6]^{32-}$
$U_{20}Pp_{10}$	$[(UO_2)_{20}(O_2)_{20}(P_2O_7)_{10}]^{40-}$
U_{20R}	$[(UO_2)_{20}(OH)_{16}(O_2)_{28}]^{32-}$
$U_{20}L_{10}$	$[(UO_2)_{20}(O_2)_{20}[(PO_3)_2C(OH)CH_3]_{10}]^{40-}$
$U_{22}P$	$[(UO_2)_{22}(O_2)_{15}(HPO_3)_{20}(H_2O)_{10}]^{26-}$
U_{24}	$[(UO_2)_{24}(OH)_{24}(O_2)_{24}]^{24-}$
$U_{24}Pp_{12}$	$[(UO_2)_{24}(O_2)_{24}(P_2O_7)_{12}]^{48-}$
$U_{24}PCP_{12}$	$[(UO_2)_{24}(O_2)_{24}(CH_2P_2O_6)_{12}]^{48-}$
U_{24R}	$[(UO_2)_{24}(O_2)_{36}(OH)_{12}]^{36-}$
$U_{24}Fe_{24}$	$[(UO_2)_{24}(FeOH)_{24}(O_2)_{24}(PO_4)_8(CH(COO)(PO_3)_2)_{24}]^{96-}$
$U_{24}L_{12}$	$[(UO_2)_{24}(O_2)_{24}[(PO_3)_2C(OH)CH_3]_{12}]^{48-}$
$U_{26}Pp_{11}$	$[(UO_2)_{26}(O_2)_{28}(P_2O_7)_{11}]^{48-}$
$U_{26}Pp_6$	$[(UO_2)_{26}(O_2)_{33}(P_2O_7)_6]^{38-}$
U_{28a}	$[(UO_2)_{28}(O_2)_{28}(OH)_{28}]^{28-}$
$U_{28}P$	$[(UO_2)_{28}(O_2)_{20}(HPO_3)_{24}(H_2O)_{12}]^{32-}$
U_{28}	$[(UO_2)_{28}(O_2)_{42}]^{28-}$
$U_{28}U_{40R}$	$[(UO_2)_{68}(O_2)_{74}(OH)_{16}(NO_3)_{16}(H_2O)_{16}]^{44-}$
$U_{28}Mo_4P_{12}$	$[(UO_2)_{28}(O_2)_{24}(MoO_3OH)_4(H_2PO_4)_{12}(H_2O)_{12}]^{20-}$
$U_{28}W_4P_{12}$	$[(UO_2)_{28}(O_2)_{24}(WO_3OH)_4(H_2PO_4)_{12}(H_2O)_{12}]^{20-}$
U_{30}	$[(UO_2)_{30}(O_2)_{36}(OH)_{22}]^{34-}$
U_{30a}	$[(UO_2)_{30}(O_2)_{30}(OH)_{30}]^{30-}$
$U_{30}Pp_6$	$[(UO_2)_{30}(O_2)_{39}(P_2O_7)_6]^{42-}$
$U_{30}Pp_{10}Ox_5$	$[(UO_2)_{30}(O_2)_{30}(P_2O_7)_{10}(C_2O_4)_5]^{50-}$

$U_{30}Pp_{12}P_1$	$[(UO_2)_{30}(O_2)_{30}(P_2O_7)_{12}(PO_4)(H_2O)_5]^{51-}$
U_{32}	$[(UO_2)_{32}(OH)_{32}(O_2)_{32}]^{32-}$
$U_{32}Pp_{16}$	$[(UO_2)_{32}(O_2)_{32}(P_2O_7)_{16}]^{64-}$
U_{32R}	$[(UO_2)_{32}(O_2)_{40}(OH)_{24}]^{40-}$
U_{36a}	$[(UO_2)_{36}(O_2)_{36}(OH)_{36}]^{36-}$
U_{36}	$[(UO_2)_{36}(O_2)_{41}(OH)_{26}]^{36-}$
$U_{36}Ox_6$	$[(UO_2)_{36}(O_2)_{48}(C_2O_4)_6]^{36-}$
$U_{38}Pp_{10}Nt_4$	$[(UO_2)_{38}(O_2)_{40}(P_2O_7)_{10}(NO_3)_4]^{56-}$
U_{40}	$[(UO_2)_{40}(OH)_{40}(O_2)_{40}]^{40-}$
$U_{40}L_{20}$	$[(UO_2)_{40}(O_2)_{40}[(PO_3)_2C(OH)CH_3]_{20}]^{80-}$
U_{42}	$[(UO_2)_{42}(O_2)_{42}(OH)_{42}]^{42-}$
$U_{42}Pp_3$	$[(UO_2)_{42}(O_2)_{42}(OH)_{36}(P_2O_7)_3]^{48-}$
U_{44}	$[(UO_2)_{44}(O_2)_{66}]^{44-}$
U_{44a}	$[(UO_2)_{44}(O_2)_{44}(OH)_{44}]^{44-}$
$U_{44}Mo_2P_{16}$	$[(UO_2)_{44}(O_2)_{38}(H_2PO_4)_{14}(HPO_4)_2(MoO_3OH)_2(OH)_{15}(H_2O)_{14}]^{23-}$
$U_{45}Pp_{23}$	$[(UO_2)_{45}(O_2)_{44}(P_2O_7)_{23}]^{90-}$
$U_{48}W_6P_{48}$	$[(UO_2)_{48}(O_2)_{12}(WO_4OH)_6(H_2PO_4)_{24}(HPO_4)_{24}]^{18-}$
$U_{48}V_6P_{48}$	$[(UO_2)_{48}(O_2)_{12}(VO_5)_6(PO_4)_{48}]^{96-}$
$U_{50}W_6P_{20}$	$[(UO_2)_{50}(O_2)_{42}(WO_3OH)_6(H_2PO_4)_{20}(OH)_8(H_2O)_{18}]^{18-}$
U_{50}	$[(UO_2)_{50}(OH)_{50}(O_2)_{50}]^{50-}$
$U_{50}Ox_{20}$	$[(UO_2)_{50}(O_2)_{43}(OH)_4(C_2O_4)_{20}]^{30-}$
U_{60}	$[UO_2(O_2)(OH)]_{60}^{60-}$
$U_{60}Ox_{30}$	$[(UO_2)_{60}(O_2)_{60}(C_2O_4)_{30}]^{60-}$
$U_{64}L_{32}$	$[(UO_2)_{64}(O_2)_{64}[(PO_3)_2C(OH)CH_3]_{32}]^{128-}$
$U_{120}Ox_{90}$	$[(UO_2)_{120}(O_2)_{120}(C_2O_4)_{90}]^{180-}$
$U_{124}P_{32}$	$[(UO_2)_{124}(O_2)_{152}(PO_4)_{16}(HPO_4)_8(H_2PO_4)_8(OH)_2(H_2O)_{24}]^{132-}$

Cage topologies

Soon after the initial discovery of uranyl peroxide cages, efforts were focused on isolating cages with peroxide and hydroxyl bridges between uranyl ions, and exploring the impact of different alkali cations and the solution pH on cluster topology.[24, 27-32] This yielded 19 uranyl peroxide clusters, of which one (U_{16}) is cup-shaped,[30] three (U_{20R}, U_{24R}, U_{32R}) are open rings (crowns),[24, 30] and 15 are cages.[19, 24, 27-31] Selected clusters are illustrated in Figure 1. Capsules with only peroxide and hydroxide bridging the uranyl ions are compositionally the simplest clusters of this family. These are the most valuable for understanding assembly mechanisms and solution speciation, and also for delineating reaction conditions that control cluster topologies. In the vast majority of these capsules, the uranyl polyhedra have two peroxide ligands, and two *cis*-hydroxide ligands: $[UO_2(O_2)_2(OH)_2]^{4-}$; or three peroxide ligands $[UO_2(O_2)_3]^{4-}$. The bridging of uranyl ions though hydroxide [UO_2-$(OH)_2$-UO_2, denoted linkage A] and peroxide [UO_2-(O_2)-UO_2, denoted linkage B] differ considerably, and this is one controlling factor of the cluster topology that will dominate in a reaction solution and eventually crystallize. For example, linkage A has a U-U distance of 3.9 Å, whereas linkage B has a U-U distance of 4.2 Å. Additionally, the internal (shortest) O_{yl} - O_{yl} distance for linkage A is 3.0 Å and this distance is 2.8 Å for linkage B, where a

shorter distance indicates a smaller dihedral angle. These differences lead to different cluster topologies, and the solution pH influences which building block dominates the solution (higher pH leads to dominance of the $[UO_2(O_2)_2(OH)_2]^{4-}$ building block).[25]

Rings of five peroxide-bridged uranyl ions (pentamers) form the U_{20} cage that contains 12 topological pentagons (pentagons in the connectivity graph) and is the smallest uranyl peroxide cluster that has a fullerene topology.[28] Addition of topological hexagons gives the fullerene-topology family consisting of U_{28}, U_{30a}, U_{36}, U_{44}, U_{50} and U_{60}. Uranyl ions arranged in four-membered rings (tetramers) are topological squares in U_{24}, the first uranyl peroxide cluster discovered. U_{24} is uniquely formed from only topological squares and hexagons, and has the sodalite topology.[19] The series U_{28a}, U_{30}, U_{32}, U_{36a}, U_{40}, and U_{42} have cages containing topological squares, pentagons, and hexagons.[31] In U_{44a}, topological squares and hexagons are combined with octagons.[31]

Uranyl peroxide cages favor high symmetry topologies. U_{60} has the highest symmetry of the 1812 fullerene topologies with 60 vertices.[29] Addition of topological squares further increases the number of possible isomers for a given number of vertices relative to fullerenes. Calculation of possible topologies within specified boundary constraints demonstrated that uranyl peroxide cages containing topological squares also strongly favor high symmetry topologies.[31] A notable and remarkable exception to the preference for high symmetry topologies in uranyl peroxide cages is $U_{45}Pp_{23}$, which has no symmetry.[33]

Introduction of diverse uranyl bridges and transition metal polyhedra

Synthetic efforts aimed to incorporate different bridges (other than peroxide or hydroxyl) between uranyl ions initially focused on pyrophosphate (Pp), which yielded 14 clusters (Table 1),[33, 34] and oxalate (Ox), for which five clusters were isolated (Table 1).[35, 36] Pyrophosphate and oxalate coordinate uranyl ions in a side-on bidentate configuration in uranyl peroxide cage clusters. Most pyrophosphate and oxalate-bearing cages are derivatives of earlier-known uranyl peroxide clusters. Oxalate in fullerene-topology $U_{50}Ox_{20}$ and $U_{60}Ox_{30}$ clusters are in the same locations as pairs of hydroxyl that were an edge of a uranyl hexagonal bipyramid in U_{50} and U_{60}.[35, 36] Pyrophosphate are in the same locations as some of the peroxide bridges of U_{20}, yielding three different cages,[34] and pairs of hydroxyl in U_{24}, giving a cage containing 12 pyrophosphate groups.[34, 37, 38] Sometimes inclusion of oxalate or pyrophosphate resulted in novel topologies, such as $U_{32}Pp_{16}$, which contains eight tetramers of uranyl ions,[34] and the core-shell $U_{120}Ox_{90}$ that features a central $U_{60}Ox_{30}$ cluster surrounded by 12 pentamers of uranyl ions that are coordinated by non-bridging oxalate groups.[35] $U_{30}Pp_{10}Ox_5$ contains both pyrophosphate and oxalate bridges between uranyl ions, in addition to peroxide. It is also worth noting that low valent uranium (U(IV)/U(V)) cluster topologies have been obtained by use of different ligands.[39,40]

Six uranyl peroxide cage clusters containing 1-hydroxyethane-1,1-diphosphonic acid ligands (L) as bridges between uranyl ions were isolated ($U_{24}L_{12}$, $U_{40}L_{20}$, $U_{64}L_{32}$, $U_{16}L_8$, $U_{20}L_{10}$, $U_{16}L_8P_4$), including one containing 64 uranyl polyhedra arranged into 16 tetramers ($U_{64}L_{32}$).[41] Despite the

geometrical similarity between this ligand and pyrophosphate, inclusion yielded four new cluster topologies. Yet another cluster with an unusual topology is a core-shell structure in which a fullerene topology U_{28} cage is surrounded by a ring consisting of 40 uranyl peroxide polyhedra and several nitrate groups ($U_{28}U_{40R}$).[42]

Transition metal polyhedra have added further topological complexity to uranyl peroxide cages. Incorporation of tungstate ($U_{18}W_2P_{12}$, $U_{28}W_4P_{12}$, $U_{50}W_6P_{20}$, $U_{48}W_6P_{48}$), molybdate ($U_{28}Mo_4P_{12}$, $U_{44}Mo_2P_{16}$), or vanadate ($U_{48}V_6P_{48}$) polyhedra as building units resulted in highly unusual topologies that include large pores in the walls in some cases and a departure from the typical topological squares, pentagons and hexagons.[43] Time-resolved studies of the solution that yielded a large uranyl vanadate cluster showed that smaller clusters, perhaps U_{24} or U_{28}, formed soon after combination of the reactants, and that these broke down after several days, followed by formation of the larger cluster.[44] In another study, uranyl peroxide clusters were synthesized that contain trimers of iron polyhedra ($U_{24}Fe_{24}$) that appear to be novel across the range of polyoxometalates.[45]

Aside from pyrophosphate, adding phosphorous to uranyl peroxide solutions as phosphate or phosphite has yielded topologically unique clusters. Combining uranyl peroxide polyhedra with phosphate produced a multi-cage super tetrahedral cluster containing 124 uranyl polyhedra and 32 phosphate ($U_{124}P_{32}$).[46] In this cluster four identical cages are arranged at the vertices of a tetrahedron, and these are further linked by more polyhedra to form a central cage.[46] Two chiral uranyl peroxide cages are built from belts of uranyl polyhedra and phosphite.[47] Whereas most uranyl polyhedra in clusters contain two peroxide defining *cis* equatorial edges of hexagonal bipyramids as discussed above, some of the uranyl polyhedra feature these two peroxide ligands in a *trans* arrangement that results in belts that are then bridged through phosphite.[47] Time-resolved SAXS showed that these clusters, which contain 22 and 28 uranyl polyhedra ($U_{22}P$, $U_{28}P$), form in solution within an hour of combining reactants, although considerable time passes before they crystallize.[47]

Neutron structures of U_{60} and $U_{24}Pp_{12}$

Owing to the high X-ray scattering efficiency of uranium, as well as disorder of counter cations in many cases, X-ray crystallographic studies typically fail to deliver the details of some of the counter cation arrangements and interstitial H_2O groups, as well as H atom positions, in crystals of uranyl peroxide cages. Part of the problem is that some cations, especially lithium, are mobile in crystals of these clusters, as shown by temperature-resolved nuclear magnetic resonance (NMR) studies.[48]

Large crystals of U_{60} and $U_{24}Pp_{12}$ were used for single-crystal neutron diffraction studies.[37, 49] Although superior resolution of H atoms and charge-balancing cations was achieved, it was still only possible to resolve cations and H_2O in close proximity to the uranyl peroxide cages, with more distant interstitial species obscured by omnipresent disorder. For U_{60}, the K cations are located below pentagons in the cage topology, where they are coordinated by five O_{Ur} oxygen atoms, and Li cations are distributed over several sites within the cage, where they are locally

ordered with respect to the orientations of H atoms of cage hydroxyl groups, which extend both into and outside the cage.[37] For $U_{24}Pp_{12}$, the neutron data showed that the terminal O atoms of the phosphate tetrahedra are unprotonated, but accept H bonds donated by nearby H_2O groups.[49]

Cluster formation mechanisms and the role of counter cations

The mechanisms for self-assembly of uranyl peroxide polyhedra in water involves base promoted peroxide decomposition, as evidenced by the release of O_2 gas during the reaction.[50] In some cases, with dependence on the counter cation, a sufficient quantity of peroxide must be decomposed in order for monomers of uranyl to link together and form capsules. For example, a lithium uranyl peroxide monomer compound, $Li_4[UO_2(O_2)_3]\cdot xH_2O$, dissolved in water will remain in the monomeric form indefinitely, and not convert to a cluster. However, a catalytic amount of Cu promotes decomposition of the peroxide, and the U_{24} capsule will form in this pH-12 solution.[26] We presume the product of metal-catalyzed decomposition of peroxide is O_2, as evidenced by observation of gas bubbles. Peroxide decomposition also occurs without a redox active metal by disproportionation of the peroxide, yielding O_2 plus OH^-, increasing the pH slightly. On the other hand, an ammonium monomer salt can never be isolated, using the same synthetic procedure that we use to isolate the lithium[51] or sodium[52] salts of uranyl peroxide monomers, because the conversion to the U_{32R} (R denotes open crown-shaped) capsule is so rapid.[24] Similarly, dissolution of an isolated potassium salt of the uranyl triperoxide monomer leads to very rapid formation of U_{28}. High yields of U_{28} are obtained if small amounts of Cs or Rb are added, along with anions that occur in the center of the capsule such as $Ta(O_2)_4^{3-}$ or $Nb(O_2)_4^{3-}$.[53] While the structure of this microcrystalline form of 'K-monomer' is not known, Dembowski et al. showed recently that it evolves in the solid-state to single-crystals of a potassium salt of uranyl triperoxide.[54] Thermochemical measurements[52] suggest the microcrystalline powder is energetically more similar to a capsule, and ongoing studies will provide further understanding. Monomers of Rb or Cs salts are yet to be isolated. Attempts to synthesize these suggest that both poor solubility and perhaps the high reactivity that we observe for the K-monomer is yet more pronounced with larger alkalis.

Density functional theory (DFT) calculations indicate that counter cations are important in the uranyl dimerization process,[50] and subtle changes in counter cations and pH favor assembly of either four or five-membered rings of uranyl polyhedra that can become topological squares and pentagons in the complete cage. DFT was used to study small building units of uranyl peroxide clusters. Simulations focused attention on dimers of uranyl ions bridged through peroxide, which invariably have a bent U-O_2-U dihedral angle in cages.[55, 56] Studies in 2010 documented a modest energetic advantage of a bent configuration when counter cations were included in the simulation, as compared to a flat dihedral angle.[55, 56] Several years later examples of uranyl dimers bridged through peroxide were isolated that had flat dihedral angles, and further DFT simulations highlighted the importance of counter cations in stabilizing the bent configuration and the formation of tetramers and pentamers of uranyl ions.[55, 57]

In general, studies of formation mechanisms of uranyl peroxide clusters are hindered by the lack of suitable NMR nuclei, the difficulty of inserting isotopic labels into peroxide, and the ease with which isotopic labels of uranyl are lost under alkaline aqueous conditions.[58] However, clearly the counter cations play an important role; in some cases, promoting very rapid capsule formation.[24] From earlier computational studies and X-ray structures of capsules that reveal alkali positions, we initially concluded that the main role of alkalis in determining cluster self-assembly and topology is templating the topological polygons.[55, 57] Specifically, we have observed and simulations show that alkali cations bind in faces of the clusters (topological polygons) that are commensurate with their size (i.e. Li in square faces, Na/K in pentagonal faces, Rb/Cs in hexagonal faces).[59, 60] However, more recent evidence suggests the location of the alkalis is adventitious,[25] and their exact role in formation mechanisms is yet to be determined.

Aside from our emerging understanding of the role of alkalis and other counterions on self-assembly processes, their influence on capsule solubility is fairly well documented. The discussion below is summarized in Figure 2. Understanding how to control dissolution, slow crystal growth, and rapid precipitation via the counter cation is crucial to manipulate and purify these clusters for solution and solid-state experiments. Typically, alkali salts of polyoxometalates follow a 'normal' solubility trend in which the order of solubility as a function of the counter cation follows the periodic trend Li>Na>K>Rb>Cs.[61] The uranyl capsules follow this trend as well.[17] The trend arises because the size and stability of hydration spheres of alkali cations increases with increased charge-density; thus, Li carries a large hydration sphere, whereas Cs^+ carries a small hydration sphere. Therefore Cs^+ can more readily bind to the capsules and bridge capsules, which leads to neutralization and aggregation. Li^+, on the other hand, is generally separated from the capsules by a hydration sphere, not allowing direct contact, and solubility is maintained.

We note that uranyl peroxide capsules are generally less soluble as alkali salts than the tungstate polyoxometalates, although they follow the same trend. For example, while K^+ is often the 'go-to' alkali for controlled crystallization of tungstate POMs, it generally provides poorer solubility for uranyl peroxide capsules, and Na^+ is a better choice. One hypothesis for this is the capsule faces provide polydentate coordination to the alkalis, similar to crown ethers, as many alkalis have been observed bound in this manner. While the alkalis coordinate to the yl oxygen atoms inside the capsules, they bind to the bridging peroxides outside the capsule. In summary, the association of alkalis with uranyl peroxide capsules may be due to more than electrostatic interactions; and strong direct bonding to the geometric faces leads to more complete neutralization, leading to precipitation.

Since charge-balancing lattice alkalis are metal cations, they are found in regular or distorted coordination polyhedra, and capsule ligands serve as apices in their polyhedral coordination. Tetraalkylammonium cations are different, in that they do not strongly associate with anions in solution. Therefore, they provide solubility for POMs including the uranyl peroxide capsules. This is true for tetramethyl and tetraethyl ammonium cations. Hydrophobic, larger alkyl groups provide poor aqueous solubility. The solubility of ammonium (NH_4^+) salts of POMs is less well

documented. Ammonium is probably not used extensively because it evaporates from solution as NH_3, and consequently increases the acidity of the solution, leading to changes in cluster speciation. Ammonium has a strong templating and precipitating effect with uranyl peroxide capsules. This is noted above concerning the rapid formation and precipitation of U_{32R}, and the inability to isolate a monomer form. This is probably due to: 1) The evaporation of NH_3, as decreasing the pH drives self-assembly. 2) Strong H-bonding of NH_4^+ to anionic capsules leads to neutralization and precipitation. Regarding the former point, it has been documented that self-assembly of capsules is accelerated by decreasing the hydroxide content of reaction solutions.[25]

While alkali cations introduced in reaction solutions play some role in uranyl peroxide cluster self-assembly, they can also be used to re-dissolve crystallized or precipitated clusters without changing the speciation, as long as the pH does not change. For example, poorly soluble K, Rb and Cs salts of uranyl capsules can be re-dissolved in TMA^+ or Li^+ electrolyte solutions.[53] This is standard practice for transition metal POMs, and has been adapted for uranyl peroxide POMs. Finally, and discussed further below, hydrophobic cations including surfactants and larger tetraalkylammonium cations can be used to rapidly precipitate uranyl peroxide capsules from water for re-dissolution in nonpolar solvents. This too was adapted from transition metal POM chemistry.[62]

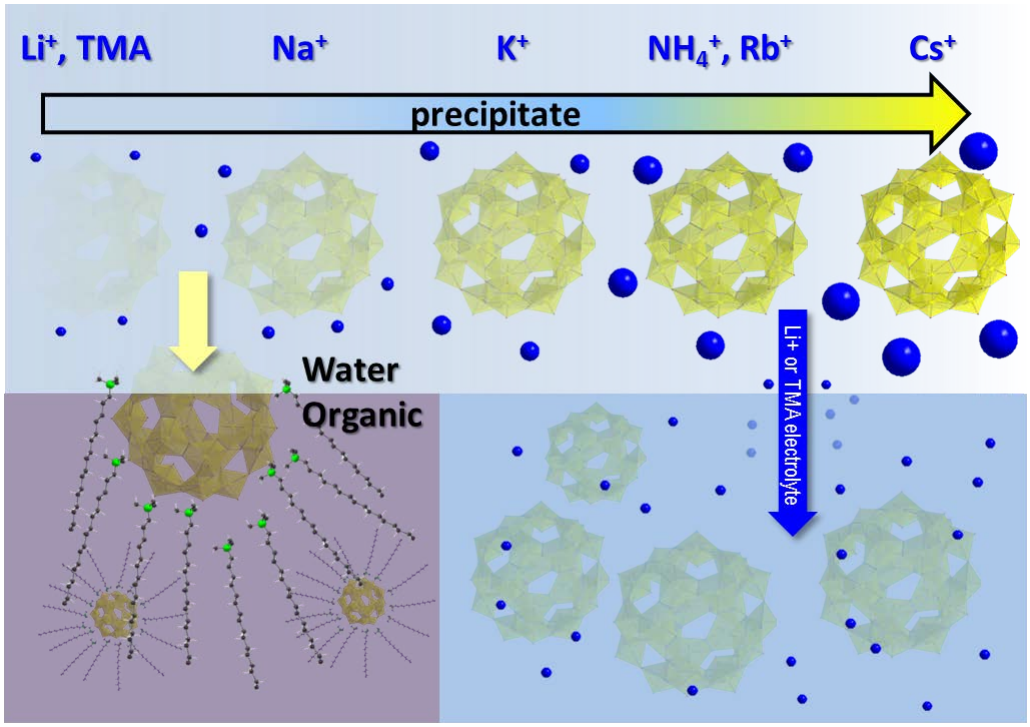

Figure 2. Schematic illustrating solution phase manipulation of uranyl peroxide (i.e. U_{28}) capsules via counter cations. **Top**: Illustrating the solubility trend as a function of counter cation: Li^+~TMA^+>Na>K>NH_4^+,Rb^+>Cs^+ (TMA=tetramethyl ammonium; blue spheres represent alkali cations). **Bottom left**: transfer of capsules dissolved in water into nonpolar immiscible solvent, using long chain surfactants. **Bottom right**: Re-dissolution of insoluble POM salts (i.e. Cs) by dissolving in electrolyte solutions (i.e. Li or TMA).

Uranyl peroxide clusters in solution

SAXS and electrospray ionization mass spectrometry (ESI-MS) provide definitive evidence that uranyl peroxide clusters form in aqueous solution before crystallization.[25, 26, 42, 44, 46, 47, 63-65] Early work focused on isolating crystals of uranyl peroxide clusters and determination of their structures by X-ray diffraction. As the library of known clusters expanded, studies of clusters in solution assumed more importance for understanding mechanisms and sequences of cluster formation, as well as transformations and dynamics in solution.[66] The vast library of structures serves a very important role in simulating solution phase data in order to identify intermediates in solution, or identify solution species when crystallization is not possible. Figure 3 summarizes both solid-state and solution characterization techniques that are valuable in studies of uranyl peroxide capsules.

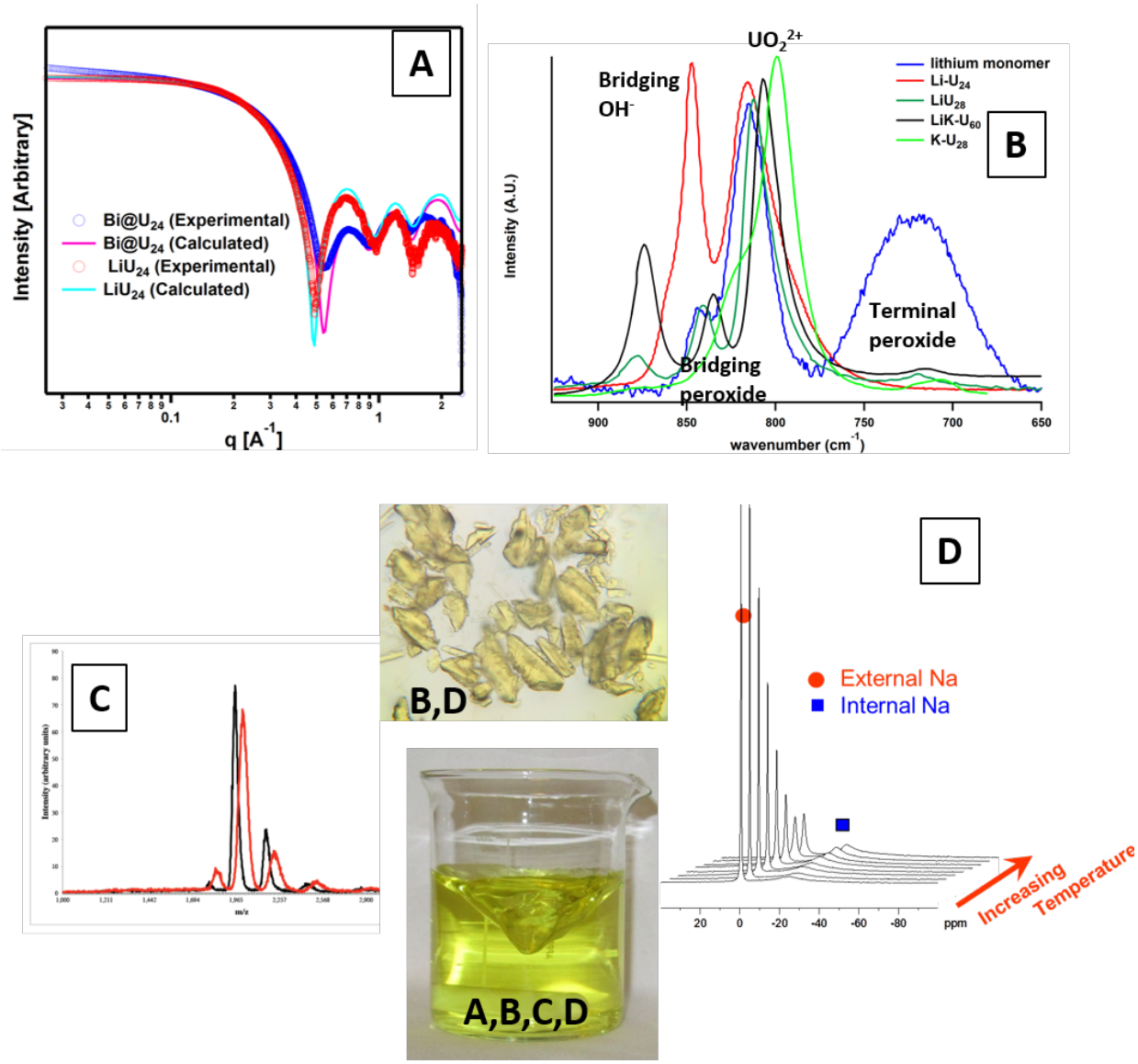

Figure 3. An overview of solution and (bulk) solid characterization most typically employed for uranyl peroxide capsules. **A.** Solution SAXS. Simulated (turquoise) and experimental (red) scattering data for Li-U_{24} showing excellent agreement out to two oscillations. Upon encapsulation of a heavy metal Bi-oxo cluster, the first oscillation is suppressed in both the experimental (blue) and simulated (pink) scattering data.[67] B. Solid and Solution Raman. Illustrating the vibrational bands that fingerprint uranyl peroxide species. A terminal peroxide ligand that typifies monomers or open capsules produces a broad peak below 750 cm^{-1} (blue). Bridging peroxides of closed capsules produces a weak peak from ~ 800 to 850 cm^{-1} (dark green, black). This peak shifts considerably as a function of capsule geometry and encapsulated species. For example, the spectrum for K-U_{28} only has a corresponding shoulder, as it overlaps with the uranyl stretch (lime green). The strong uranyl stretch is observed in every spectrum around 800 cm^{-1}. C. Solution ESI-MS This technique is less frequently employed, but in this illustration, we observe several broad peaks of U_{60} as a K/Li salt (black). Upon addition of Cs (red), these peaks shift to higher m/z (mass/charge). D. Solution and solid-state NMR. Example of ^{23}Na NMR of Cs/Na-U_{28} in solution represents one type of experiment that is possible. Two peaks correspond with encapsulated (broad, -20 ppm) and free (sharp, 0 ppm) Na^+. Heating the solution increases the exchange rate, and exchange kinetics can be determined.[68]

SAXS provides information on the size of uranyl peroxide cages in solution. In fact, the uranyl peroxide capsules yield 'textbook' SAXS data, due to both the strong scattering power of the uranium atom, and the pronounced oscillations that arise from the capsule topology (Figure 3A).[69] ESI-MS provides mass/charge information, although signals are extremely broad, of very high m/z, and difficult to interpret (Figure 3C).[63] This may be partly due to instability of the peroxide ligand during the ionization process. Raman spectroscopy yields strong uranyl, hydroxide and peroxide vibrations from cluster-bearing solutions, with subtle changes in the spectra attributable to different cluster topologies in some cases (Figure 3B).[63] Raman spectra differentiate between closed capsule forms and monomers or open capsules, based on the absence or presence of terminal peroxides, respectively. Dynamic and static light scattering allow detection of uranyl peroxide clusters in solution, and more importantly, size distributions for aggregates of clusters.[70-73] For clusters containing appropriate nuclei in either the counter cations or capsule framework, nuclear magnetic resonance (NMR) spectroscopy has allowed characterization of clusters in solution. These include ^{1}H, ^{31}P, [48, 66, 74] ^{6,7}Li,[37, 48, 75] ^{133}Cs,[68] and ^{23}Na (example in Figure 3D).[68] A single study has demonstrated that U_{60} clusters and their aggregates can be resolved by cryogenic transmission electron microscopy (cryo-TEM), and this reveals their distribution and shapes at the instant when the solution was fused into glass.[76] This technique could become extremely powerful in the future as it becomes more widely available for determining cluster topologies that cannot be crystallized, or for determining aggregation pathways.

Spectroscopic data in combination with SAXS and single-crystal X-ray data has provided fascinating details of cluster evolution in aqueous solution that reveal breakdown and assembly of new cages as a function of changing conditions (Figure 4).[74] For example, when uranyl nitrate, lithium hydroxide, hydrogen peroxide, pyrophosphate, and water are combined, yielding alkaline conditions, U_{24} rapidly assembles in solution.[38] Subsequently, titrating in oxalic acid results in the destruction of U_{24}, which fragments to at least the level of uranyl tetramers, and reassembly into the topologically related $U_{24}Pp_{12}$ cage.[38] Further reduction of the pH results in fragmentation of $U_{24}Pp_{12}$ and assembly of the larger $U_{32}Pp_{16}$ cage, which is sparingly soluble under the mildly acidic aqueous conditions of its formation.[74]

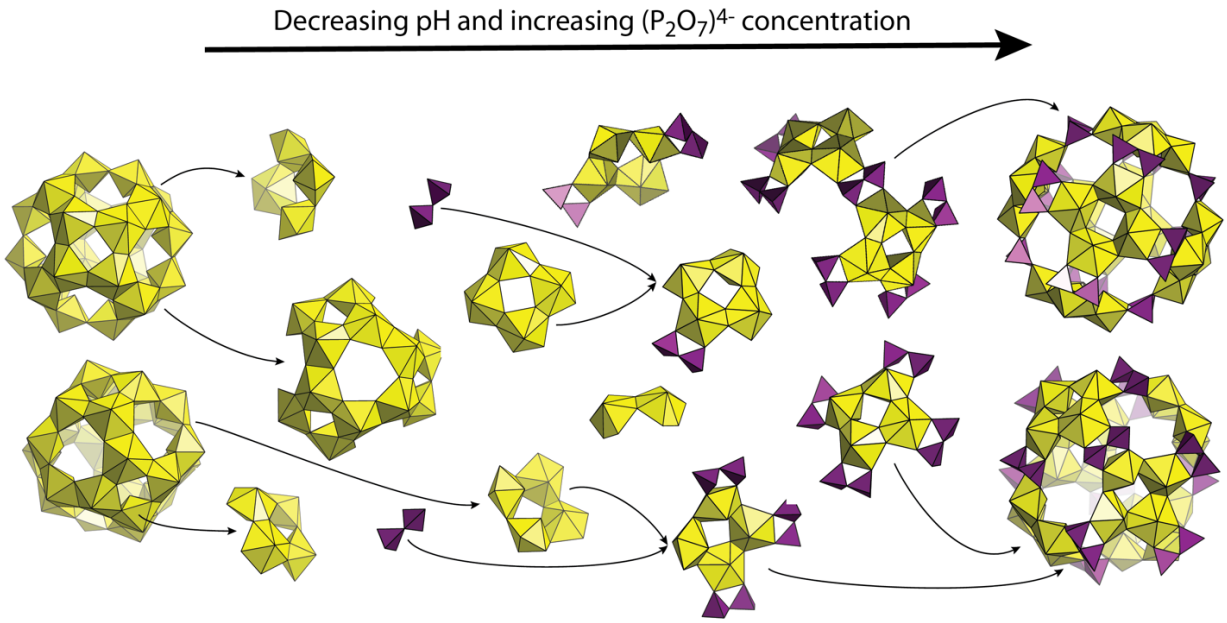

Figure 4. Proposed pathway of conversion of U_{24} to the related $U_{24}Pp_{12}$.

As mentioned above, recent studies indicate that the presence and concentration of alkali cations are not the only parameters that control cluster topology. It was demonstrated that pH also influences cluster topology,[13] where higher pH favors topologies with hydroxyl ligands, and lower pH favors topologies with peroxide-only ligands. SAXS and Raman spectroscopy were combined to examine the formation of uranyl peroxide clusters in an aqueous LiOH solution[25] where the LiOH/U ratio was carefully controlled. When the solution corresponded to a LiOH/U ratio of around three, U_{28} formed in less than a day and could be produced in high yield.[25] With aging of this solution, after 15 days U_{24} also appeared in solution. For solutions with LiOH/U ratios of four and five and greater, the monomer always formed first, which would evolve to U_{24} with solution aging (stored in a loosely capped vial in ambient conditions), and the time delay of U_{24} formation increased with the LiOH/U ratio. The mechanism is not well-understood. The time delay to cluster formation is most likely required for adequate decomposition of the peroxide to a level where the monomer is no longer supported. In most cluster forms; the peroxide to uranium ratio is <2. On the other hand, the ratio is exactly 3 for the monomer form. Other counter cations likewise produced U_{28} when minimal hydroxide was used, with solutions around pH-10. The utility of SAXS was exemplified in this study, in that subtle differences between similar sized U_{24} and U_{28} produced marked changes in the scattering data. This study also reveals a more complex conversion of topologies, unlike the envisioned conversion of U_{24} to $U_{24}Pp_{12}$. Specifically, U_{24} consists of topological squares and hexagons, whereas U_{28} consists of pentagons and hexagons. SAXS also indicated that the transformation between these clusters happens without complete breakdown of the clusters. Rather, it occurs via substitution of ligands while the cluster remains intact. For example, as peroxide ligands are replaced by dihydroxide ligands, the cluster distorts, followed by rapid rearrangement.

Studies of the aqueous solubility of crystals of U_{60} and $U_{24}Pp_{12}$ showed that they readily dissolve when placed in neat water and that the pH of the solution drifts to about 10 in the case of U_{60}.[77] SAXS and ESI-MS showed the clusters remain intact in solution, and that they assume an approximately closest packed arrangement with cluster concentrations reaching as high as 1.8 moles of U per kg of water.[77] The maximum U content in solution was achievable from Li-based cluster crystals, as compared to Na and K-bearing crystals (Figure 2), reflecting the importance of the counter cations in determining cluster solubility.[77] Molecular dynamics simulations of U_{60} indicate that the population of Li and K cations inside and near the outside of the cage is cluster concentration dependent, and that at very high cluster concentrations in solution more cations move through the pores into the cages.[77]

NMR studies of ^{31}P in $U_{24}Pp_{12}$ yielded identical diffusion coefficients for the two distinct P sites in the cluster, demonstrating cluster stability.[66] Heating the cluster-bearing solution while collecting NMR data indicated dynamic interchange of cluster isomers involving flexing of the cage, and stability to 65 °C, above which breakdown products appeared.[66] ESI-MS studies of a solution of U_{60} over several months also demonstrated cluster stability.[52] Crystals of U_{60} subjected to extreme pressures in a diamond anvil cell became X-ray amorphous, but ESI-MS of a solution containing the quenched material demonstrated that U_{60} clusters survived intact.[78]

While all uranyl peroxide cluster capsules reported thus far are formed and crystallized from water, there is great utility to transferring these clusters to non-aqueous media (Figure 2). Transferring primarily water-stable clusters to non-aqueous solvent stabilizes clusters that are normally subject to alteration via hydrolysis reactions. It allows us to carry out chemical experiments otherwise not possible in aqueous media, i.e. organic ligand functionalization. In the case of capsule topologies, it provides an opportunity for completely different behavior of encapsulated species. Transition metal POM chemistry has been well-adapted for non-aqueous chemistry. Clusters can be transferred into organic media simply by solvent extraction. In this process, a solvent that is immiscible with water and contains a hydrophobic salt is contacted with an aqueous solution of the cluster. Ideally, the cluster transfers into the organic phase via ion exchange. This is typically done in POM chemistry, for example, by employing a non-aqueous solution of tetrabutylammonium or tetraheptylammonium chloride. The chloride is transferred to the aqueous phase, while the POM in transferred to the non-aqueous phase to maintain charge-balance. The driving forces for exchanges such as these are energetics of solvation of ions in the disparate phases, and the relatively low charge density of the clusters makes the transfer possible.

We have developed a non-aqueous solvent system consisting of cetyltrimethylammonium bromide (surfactant) in kerosene that readily extracts uranyl peroxide capsules.[75] This chemistry yielded opportunity for both new fundamental studies of the encapsulated species and an atom efficient uranium separations process (discussed below). In one study, we extracted U_{24} clusters containing encapsulated Li. Encapsulated Li cannot be resolved by Li-NMR in U_{24} in aqueous media or in solids with lattice water, due to extremely rapid exchange of Li between the capsule and the aqueous medium or water-containing lattice. On the other hand, Li NMR analysis of a kerosene solution containing U_{24} with encapsulated lithium reveals

multiple, extremely sharp peaks with chemical shift values that indicate encapsulated Li. This is consistent with lithium becoming immobilized and isolated inside the capsules, away from its hydrophobic surroundings upon dissolution in kerosene. Current studies are focused on utilizing computational and more detailed NMR studies to determine the exact coordination environments that give rise to the different chemical shifts. Less well understood is the origin of the very narrow peaks in the spectra. Normally, narrow peaks indicate rapid motion in solution, which is *inconsistent* with encapsulation. This might suggest unique tumbling behavior of the capsule within the surfactant shell. This too is a subject of future investigation, and potentially represents a unique macromolecular physical phenomenon.

Supramolecular assembly of clusters

Pioneering work by Liu demonstrated that anionic transition metal polyoxometalates undergo cation-mediated assembly into vesicle-like structures referred to as blackberries.[79-82] Uranyl peroxide cages also form blackberries in solution, with resulting diameters in the range of a few tens of nanometers, that have been characterized using a combination of light and X-ray scattering techniques (Fig. 5).[70] Temperature and cation dependence of blackberry size indicates that some cations are able to pass through the pores of uranyl peroxide cages in solution, allowing the overall cluster to modify its charge. Taking advantage of the high electron density of uranyl peroxide clusters, cryogenic transmission electron microscopy was used to image fully formed blackberries built from U_{60} that formed within 30 minutes of adding additional cations to U_{60} solutions, as well as time-resolved intermediates of blackberry formation (Fig. 5).[76]

A very recent study focused on characterizing nuclear waste contained in Cold War era underground storage tanks at Hanford, Washington (U.S.A.) identified spherical strontium-rich uranium particles with diameters in the range of 10s of nanometers.[83] These storage tanks contain 56 million gallons of waste, the remediation of which is expected to cost $16B USD.[83] The authors noted the similar dimensions and appearance in transmission electron microscope images of the uranium-rich particles found in the tanks and uranyl peroxide nanoclusters,[83] specifically the blackberries made of U_{60} characterized earlier by cryogenic transmission electron microscopy.[76] These findings suggest the importance of uranyl peroxide clusters in nuclear wastes and the environmental transport of radionuclides.

Thermodynamics of uranyl peroxide cluster compounds

High-temperature drop-solution calorimetry has provided enthalpies of formation of a few uranyl peroxide cage compounds.[52, 84] The general conclusion of these studies is that the charge-balancing alkali cations and their electrostatic interactions with the anionic clusters dominate in determining the energetic stability of the overall cluster-bearing crystals.[84] Logically it follows, and experiments show that the uranyl peroxide monomers have a more negative enthalpy of formation than the capsules, because they have more alkali-anion interactions per uranyl than the capsules. On the other hand, calorimetric studies of solid forms of uranyl peroxide clusters provide only limited insight into the relative energetics of cages that

differ in size and topology. Kinetics and reaction pathways may play a more important role in determining cluster topology. Indeed, all clusters are kinetic intermediates to thermodynamically stable phases, and therefore provide valuable insight into reactive pathways to metal oxide materials in water.

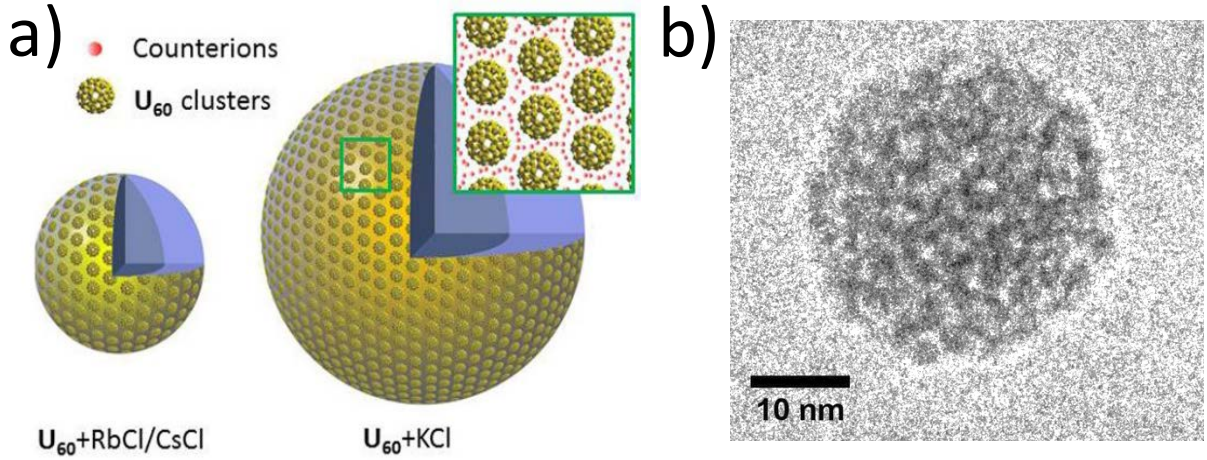

Figure 5. Schematic of two different sized blackberries constructed from U_{60} (a),[71,72] and an image of a U_{60} blackberry with Ca counter cations collected at cryogenic temperature in a transmission electron microscope.[76]

Endohedral clusters, beyond alkali encapsulation

One great challenge of uranyl peroxide capsules (and broadly many cluster chemistries) is synthesizing heterometallic clusters. For the capsules, this can mean either substitution within the shell or inside the cage by transition metals, main group metals or other f-elements. Both present the same challenges including 1) identifying pH ranges that provide solubility and promote hydrolysis and condensation reactions of uranyl and the heterometal, and 2) limiting and/or exploiting heterometal-promoted decomposition of the peroxide. Heterometal substitution in the cage has been discussed prior in this review and includes W, V and Fe. Endohedral clusters of $[Bi_6O_8]^{2+}$ and $[Pb_8O_6]^{4+}$ polycations encapsulated in U_{24} cages has also been achieved. These results are particularly fascinating, because both bismuth and lead are notoriously insoluble in any aqueous conditions aside from highly acidic. Therefore, we assume that the assembly process occurs heterogeneously at the solid surface of bismuth and lead oxide powders, and the endohedral clusters are encapsulated intact rather than exchanged-in as cations. The bridging oxo ligands also supports this hypothesis.[67] In contrast, encapsulated polycationic species containing Ca, Sr or Ba are instead bridged by water molecules, suggesting these enter the capsule after it is assembled. In other words, the uranyl capsule templates the endohedral cluster. However, similarly, solubility of the alkaline earth metals is enabled in base in these complex reaction mixtures.[85]

Applications

The nuclear fuel cycle relies on methods for separating and purifying uranium from complex geochemical matrices at the front end of the cycle, and from highly radioactive irradiated fuel containing one-third of the periodic table at the back-end of the cycle. Typically, irradiated fuel processing involves dissolution of the fuel in nitric acid, followed by solvent extraction using hydrocarbons. Recent studies demonstrated that UO_2 is soluble in mildly alkaline water containing substantial hydrogen peroxide that was added to the solution, and that uranyl peroxide cage clusters result. U_{24} and U_{32} clusters were the focus of these studies.[64, 65,75] This was demonstrated using simulated spent nuclear fuel that contained non-radioactive isotopes of selected fission products including rare earths, alkalis, alkaline earths, and transition metals in addition to uranium (>90%). Following dissolution, the clusters that assembled in solution were separated from some of the other species in solution on the basis of filtration through porous membranes,[64, 65] or by solvent extraction as discussed above.[75] Separation of some fission products is enabled simply by poor solubility in base, especially for the lanthanides. Other elements, such as alkalis and alkaline earths, were co-extracted with the capsules, and encapsulation or ion-association might be the origin of this. We also demonstrated that extraction of acidic clusters formed with oxalate ligands ($(U_{60}Ox_{30}$, pH~4) was possible, further highlighting the broad utility of this process for fundamental and applied studies.

We describe the cluster based separation technologies, both solvent extraction and filtration, as 'atom efficient' because the clusters allow transfer of up to 60 uranyl ions at a time, instead of as monomer species. For example, the solvent extraction process requires less than one extractant molecule per uranyl ion. This is compared to the commonly employed UREX process in which each uranyl ion is extracted by covalent binding to two tributylphosphate ligands.

As has been a theme throughout this review, the counter cations are extremely important to understand the fundamental chemistry of uranyl peroxide capsules, and they are also important to consider for developing applications. Clusters U_{28}, U_{44}, and U_{32R} were synthesized using ammonium as the counter cation.[86] Such preparations may be important in nuclear fuel cycle applications that often include ammonium, which can be removed by heating. The same researchers demonstrated that ammonium cations contained in U_{32R} are exchangeable for Nd or Th in the solid state,[87] which may have important applications that include production of precursor materials for fuel cycle applications. For example, exchange of Pu(IV) into the uranyl peroxide clusters could provide nano-scale compositional control for fabrication of mixed oxide (MOX) fuels, and calcination of $Np@U_{32R}$ at 1400 °C yielded a pure fluorite-structure oxide.[87]

Future Directions

The energy landscape of uranyl peroxide clusters is undoubtedly complex, but information concerning the thermodynamics of cluster assembly and crystallization is currently lacking. There is a need for calorimetric measurements of energies of crystallization (or dissolution), as well as cluster assembly, so that ion association energies can be delineated from the energy of cluster self-assembly. Experimental determinations of cluster formation energetics would then

afford direct comparison with DFT computational models, and development of an understanding of the subtle energetic effects that favor specific cluster sizes and topologies.

Although significant progress has recently been realized towards a deeper understanding, there remains much uncertainty concerning the self-assembly mechanisms of uranyl peroxide cages, and the presumably subtle impacts of counter cations and pH on these processes. Recent data shows that clusters in solution sometimes respond to changing conditions by fragmenting followed by assembly of new clusters. This too would benefit from computational investigations, as well as identifying metastable intermediates to full capsule assemblies. Isolation of these intermediates that may include dimers or units containing four to six uranyl ions arranged in rings that may correspond to topological polygons in the clusters would provide opportunity to identify and control reaction pathways to known cluster topologies, and discover pathways to yet unknown cluster topologies by exploiting these intermediates as building blocks for capsule assembly.

An important characteristic of POM chemistry that has been widely exploited is the rich, reversible redox chemistry leading to applications in colorimetric detection, catalysis and energy storage. This is not yet realized for the uranyl capsules, due in part to the irreversible destruction of peroxide ligands upon electrochemical reduction.[57] However, one uranyl vanadate capsule has been identified that does not have peroxide ligands.[88] There is a need to identify other synthetic strategies to form uranyl capsules that contain no peroxide, and to determine if redox activity is achievable. Another challenge of redox activity for uranyl capsules is the loss of the uranyl unit upon addition of two valence electrons to U(VI). U^{IV} with two valence electrons does not include yl oxygen atoms in its coordination environment. There is evidence that U^{V} forms $(UO_2)^{+}$ uranyl ions and that the corresponding polyhedra can form a layered motif in a mixed U^{VI}/U^{V} compound.[89] This suggests U^{VI}/U^{V} clusters could also be attainable, and has recently been reported for non-peroxide clusters.[90] It is notable that tetravalent uranium has its own unique cluster topology, albeit requiring organic ligation.[91, 92] Therefore, one might design cluster-to-cluster transformation chemistries in solution by electrochemical synthesis.

Other largely unexplored directions include expanding this chemistry to neptunyl[19] or plutonyl capsule assembly, and using the capsules as building blocks to covalently linked materials. It will be particularly interesting to compare properties of neptunyl peroxide cages with those of uranyl, as uranyl contains no 5*f* electrons, whereas neptunyl has either one or two 5*f* electrons. The only report of a neptunyl peroxide cluster raises the possibility that the cluster contains a mixture of Np(V) and Np(VI) oxidation states.[19]

Given that uranyl peroxide clusters significantly extend the size, complexity, and properties of uranyl species in aqueous systems, and that most aspects of chemical processing in the nuclear fuel cycle utilize aqueous systems, further development of applications is warranted. There is potential to harness uranyl peroxide clusters to control the distribution of uranium between aqueous and solid phases, to separate aqueous species on the basis of size, and to solubilize other normally insoluble cations by encapsulation. The extent to which the unintended

formation of uranyl peroxide clusters occurs in nuclear waste and nuclear accident scenarios is unknown, and no studies have addressed the behavior and fate of such clusters in the environment.

Studies of uranyl peroxide clusters have come a long way from the initial identification of structures via single-crystal growth. Achievements now include controlled growth and transformation of clusters, vast topological and compositional diversities, supramolecular assemblies in solution, and a more detailed understanding of counter cation behavior. Despite twelve years of study by a growing cadre of research groups, there is still much to be discovered about the uranyl peroxide capsules, and huge potential for expansion of this family of POMs.

Acknowledgments

This research is funded by the Office of Basic Energy Sciences of the U.S. Department of Energy as part of the Materials Science of Actinides Energy Frontier Research Center (DE-SC0001089).

References

1. M. Aureliano and R. M. C. Gandara, *Journal of Inorganic Biochemistry*, 2005, **99**, 979-985.
2. A. Bijelic and A. Rompel, *Coordination Chemistry Reviews*, 2015, **299**, 22-38.
3. I. S. Lee, J. R. Long, S. B. Prusiner and J. G. Safar, *Journal of the American Chemical Society*, 2005, **127**, 13802-13803.
4. J. T. Rhule, C. L. Hill and D. A. Judd, *Chemical Reviews*, 1998, **98**, 327-357.
5. K. Stroobants, E. Moelants, H. G. T. Ly, P. Proost, K. Bartik and T. N. Parac-Vogt, *Chemistry-a European Journal*, 2013, **19**, 2848-2858.
6. L. B. Fullmer, R. H. Mansergh, L. N. Zakharov, D. A. Keszler and M. Nyman, *Crystal Growth & Design*, 2015, **15**, 3885-3892.
7. R. H. Mansergh, L. B. Fullmer, D. H. Park, M. Nyman and D. A. Keszler, *Chemistry of Materials*, 2016, **28**, 1553-1558.
8. D. A. Marsh, S. Goberna-Ferron, M. K. Baumeister, L. N. Zakharov, M. Nyman and D. W. Johnson, *Dalton Transactions*, 2017, **46**, 947-955.
9. S. Hartung, N. Bucher, H. Y. Chen, R. Al-Oweini, S. Sreejith, P. Borah, Y. Zhao, U. Kortz, U. Stimming, H. E. Hoster and M. Srinivasan, *Journal of Power Sources*, 2015, **288**, 270-277.
10. H. D. Pratt, N. S. Hudak, X. K. Fang and T. M. Anderson, *Journal of Power Sources*, 2013, **236**, 259-264.
11. H. X. Tang, F. Xiao and D. S. Wang, *Advances in Colloid and Interface Science*, 2015, **226**, 78-85.
12. J. W. Bennett, J. L. Bjorklund, T. Z. Forbes and S. E. Mason, *Inorganic Chemistry*, 2017, **56**, 13014-13028.
13. D. L. Long, E. Burkholder and L. Cronin, *Chemical Society Reviews*, 2007, **36**, 105-121.
14. D. L. Long, R. Tsunashima and L. Cronin, *Angewandte Chemie-International Edition*, 2010, **49**, 1736-1758.

15. B. L. Phillips, W. H. Casey and M. Karlsson, *Nature*, 2000, **404**, 379-382.
16. W. H. Casey, J. R. Rustad and L. Spiccia, *Chemistry-a European Journal*, 2009, **15**, 4496-4515.
17. M. Nyman and P. C. Burns, *Chemical Society Reviews*, 2012, **41**, 7354-7367.
18. J. Qiu and P. C. Burns, *Chemical Reviews*, 2013, **113**, 1097-1120.
19. P. C. Burns, K. A. Kubatko, G. Sigmon, B. J. Fryer, J. E. Gagnon, M. R. Antonio and L. Soderholm, *Angewandte Chemie-International Edition*, 2005, **44**, 2135-2139.
20. L. Cronin, *Angewandte Chemie-International Edition*, 2006, **45**, 3576-3578.
21. A. Muller, S. Sarkar, S. Q. N. Shah, H. Bogge, M. Schmidtmann, S. Sarkar, P. Kogerler, B. Hauptfleisch, A. X. Trautwein and V. Schunemann, *Angewandte Chemie-International Edition*, 1999, **38**, 3238-3241.
22. C. Schaffer, A. Merca, H. Bogge, A. M. Todea, M. L. Kistler, T. B. Liu, R. Thouvenot, P. Gouzerh and A. Muller, *Angewandte Chemie-International Edition*, 2009, **48**, 149-153.
23. A. M. Todea, A. Merca, H. Bogge, T. Glaser, J. M. Pigga, M. L. K. Langston, T. B. Liu, R. Prozorov, M. Luban, C. Schroder, W. H. Casey and A. Muller, *Angewandte Chemie-International Edition*, 2010, **49**, 514-519.
24. G. E. Sigmon and P. C. Burns, *Journal of the American Chemical Society*, 2011, **133**, 9137-9139.
25. C. Falaise and M. Nyman, *Chemistry-a European Journal*, 2016, **22**, 14678-14687.
26. Z. L. Liao, T. Deb and M. Nyman, *Inorganic Chemistry*, 2014, **53**, 10506-10513.
27. T. Z. Forbes, J. G. McAlpin, R. Murphy and P. C. Burns, *Angewandte Chemie-International Edition*, 2008, **47**, 2824-2827.
28. G. E. Sigmon, J. Ling, D. K. Unruh, L. Moore-Shay, M. Ward, B. Weaver and P. C. Burns, *Journal of the American Chemical Society*, 2009, **131**, 16648-16649.
29. G. E. Sigmon, D. K. Unruh, J. Ling, B. Weaver, M. Ward, L. Pressprich, A. Simonetti and P. C. Burns, *Angewandte Chemie-International Edition*, 2009, **48**, 2737-2740.
30. G. E. Sigmon, B. Weaver, K. A. Kubatko and P. C. Burns, *Inorganic Chemistry*, 2009, **48**, 10907-10909.
31. D. K. Unruh, A. Burtner, L. Pressprich, G. E. Sigmon and P. C. Burns, *Dalton Transactions*, 2010, **39**, 5807-5813.
32. P. C. Burns, *Mineralogical Magazine*, 2011, **75**, 1-25.
33. J. Ling, J. Qiu, J. E. S. Szymanowski and P. C. Burns, *Chemistry-a European Journal*, 2011, **17**, 2571-2574.
34. J. Ling, J. Qiu, G. E. Sigmon, M. Ward, J. E. S. Szymanowski and P. C. Burns, *Journal of the American Chemical Society*, 2010, **132**, 13395-13402.
35. J. Ling, J. Qiu and P. C. Burns, *Inorganic Chemistry*, 2012, **51**, 2403-2408.
36. J. Ling, C. M. Wallace, J. E. S. Szymanowski and P. C. Burns, *Angewandte Chemie-International Edition*, 2010, **49**, 7271-7273.
37. T. A. Olds, M. Dembowski, X. Wang, C. Hoffman, T. M. Alam, S. Hickam, K. L. Pellegrini, J. He and P. C. Burns, *Inorganic Chemistry*, 2017, **56**, 9676-9683.
38. M. Dembowski, C. A. Colla, S. Hickam, A. F. Oliveri, J. E. S. Szymanowski, A. G. Oliver, W. H. Casey and P. C. Burns, *Inorganic Chemistry*, 2017, **56**, 5478-5487.
39. B. Biswas, V. Mougel, J. Pecaut and M. Mazzanti, *Angewandte Chemie-International Edition*, 2011, **50**, 5745-5748.

40. G. Nocton, F. Burdet, J. Pecaut and M. Mazzanti, *Angewandte Chemie-International Edition*, 2007, **46**, 7574-7578.
41. Z. L. Liao, J. Ling, L. R. Reinke, J. E. S. Szymanowski, G. E. Sigmon and P. C. Burns, *Dalton Transactions*, 2013, **42**, 6793-6802.
42. J. Qiu, J. Ling, A. Sui, J. E. S. Szymanowski, A. Simonetti and P. C. Burns, *Journal of the American Chemical Society*, 2012, **134**, 1810-1816.
43. J. Ling, F. Hobbs, S. Prendergast, P. O. Adelani, J. M. Babo, J. Qiu, Z. H. Weng and P. C. Burns, *Inorganic Chemistry*, 2014, **53**, 12877-12884.
44. J. Qiu, M. Dembowski, J. E. S. Szymanowski, W. C. Toh and P. C. Burns, *Inorganic Chemistry*, 2016, **55**, 7061-7067.
45. J. Qiu, S. N. Dong, J. E. S. Szymanowski, M. Dobrowolska and P. C. Burns, *Inorganic Chemistry*, 2017, **56**, 3738-3741.
46. J. Qiu, J. Ling, L. Jouffret, R. Thomas, J. E. S. Szymanowski and P. C. Burns, *Chemical Science*, 2014, **5**, 303-310.
47. J. Qiu, K. Nguyen, L. Jouffret, J. E. S. Szymanowski and P. C. Burns, *Inorganic Chemistry*, 2013, **52**, 337-345.
48. T. M. Alam, Z. L. Liao, L. N. Zakharov and M. Nyman, *Chemistry-a European Journal*, 2014, **20**, 8302-8307.
49. M. Dembowski, T. A. Olds, K. L. Pellegrini, C. Hoffmann, X. P. Wang, S. Hickam, J. H. He, A. G. Oliver and P. C. Burns, *Journal of the American Chemical Society*, 2016, **138**, 8547-8553.
50. P. Miro, B. Vlaisavljevich, A. Gil, P. C. Burns, M. Nyman and C. Bo, *Chemistry-a European Journal*, 2016, **22**, 8571-8578.
51. M. Nyman, M. A. Rodriguez and C. F. Campana, *Inorganic Chemistry*, 2010, **49**, 7748-7755.
52. C. R. Armstrong, M. Nyman, T. Shvareva, G. E. Sigmon, P. C. Burns and A. Navrotsky, *Proceedings of the National Academy of Sciences of the United States of America*, 2012, **109**, 1874-1877.
53. M. Nyman, M. A. Rodriguez and T. M. Alam, *European Journal of Inorganic Chemistry*, 2011, **14**, 2197-2205.
54. M. Dembowski, V. Bernales, J. E. Qiu, S. Hickam, G. Gaspar, L. Gagliardi and P. C. Burns, *Inorganic Chemistry*, 2017, **56**, 1574-1580.
55. P. Miro, S. Pierrefixe, M. Gicquel, A. Gil and C. Bo, *Journal of the American Chemical Society*, 2010, **132**, 17787-17794.
56. B. Vlaisavljevich, L. Gagliardi and P. C. Burns, *Journal of the American Chemical Society*, 2010, **132**, 14503-14508.
57. A. Gil, D. Karhanek, P. Miro, M. R. Antonio, M. Nyman and C. Bo, *Chemistry-a European Journal*, 2012, **18**, 8340-8346.
58. D. L. Clark, S. D. Conradson, R. J. Donohoe, D. W. Keogh, D. E. Morris, P. D. Palmer, R. D. Rogers and C. D. Tait, *Inorganic Chemistry*, 1999, **38**, 1456-1466.
59. P. Miro and C. Bo, *Inorganic Chemistry*, 2012, **51**, 3840-3845.
60. P. Miro, B. Vlaisavljevich, A. L. Dzubak, S. X. Hu, P. C. Burns, C. J. Cramer, R. Spezia and L. Gagliardi, *Journal of Physical Chemistry C*, 2014, **118**, 24730-24740.
61. M. Nyman, *Dalton Transactions*, 2011, **40**, 8049-8058.

62. D. G. Kurth, P. Lehmann, D. Volkmer, H. Colfen, M. J. Koop, A. Muller and A. Du Chesne, *Chemistry-a European Journal*, 2000, **6**, 385-393.
63. B. T. McGrail, G. E. Sigmon, L. J. Jouffret, C. R. Andrews and P. C. Burns, *Inorganic Chemistry*, 2014, **53**, 1562-1569.
64. E. M. Wylie, K. M. Peruski, S. E. Prizio, A. N. A. Bridges, T. S. Rudisill, D. T. Hobbs, W. A. Phillip and P. C. Burns, *Journal of Nuclear Materials*, 2016, **473**, 125-130.
65. E. M. Wylie, K. M. Peruski, J. L. Weidman, W. A. Phillip and P. C. Burns, *Acs Applied Materials & Interfaces*, 2014, **6**, 473-479.
66. R. L. Johnson, C. A. Ohlin, K. Pellegrini, P. C. Burns and W. H. Casey, *Angewandte Chemie-International Edition*, 2013, **52**, 7464-7467.
67. O. Renier, C. Falaise, H. Neal, K. Kozma and M. Nyman, *Angewandte Chemie-International Edition*, 2016, **55**, 13480-13484.
68. M. Nyman and T. M. Alam, *Journal of the American Chemical Society*, 2012, **134**, 20131-20138.
69. M. Nyman, *Coordination Chemistry Reviews*, 2016, 10.1016/j.ccr.2016.1011.1014.
70. D. Li, S. Simotwo, M. Nyman and T. B. Liu, *Chemistry-a European Journal*, 2014, **20**, 1683-1690.
71. Y. Y. Gao, F. Haso, J. E. S. Szymanowski, J. Zhou, L. Hu, P. C. Burns and T. B. Liu, *Chemistry-a European Journal*, 2015, **21**, 18785-18790.
72. Y. Y. Gao, J. E. S. Szymanowski, X. Y. Sun, P. C. Burns and T. B. Liu, *Angewandte Chemie-International Edition*, 2016, **55**, 6887-6891.
73. Y. Gao, M. Dembowski, J. E. S. Szymanowski, W. Yin, S. S. C. Chuang, P. C. Burns and T. Liu, 2017, **23**, 7915-7919.
74. M. Dembowski, C. A. Colla, P. Yu, J. Qiu, J. E. S. Szymanowski, W. H. Casey and P. C. Burns, *Inorganic Chemistry*, 2017, **56**, 9602-9608.
75. H. A. Neal, J. Szymanowski, J. B. Fein, P. C. Burns and M. Nyman, *European Journal of Inorganic Chemistry*, 2017, **2017**, 39-46.
76. J. A. Soltis, C. M. Wallace, R. L. Penn and P. C. Burns, *Journal of the American Chemical Society*, 2016, **138**, 191-198.
77. K. M. Peruski, V. Bernales, M. Dembowski, H. L. Lobeck, K. L. Pellegrini, G. E. Sigmon, S. Hickam, C. M. Wallace, J. E. S. Szymanowski, E. Balboni, L. Gagliardi and P. C. Burns, *Inorganic Chemistry*, 2017, **56**, 1333-1339.
78. K. M. Turner, J. E. S. Szymanowski, F. Zhang, Y. Lin, B. T. McGrail, W. L. Mao, P. C. Burns and R. C. Ewing, *Journal of Materials Research*, 2017, **32**, 3679-3688.
79. M. L. Kistler, A. Bhatt, G. Liu, D. Casa and T. B. Liu, *Journal of the American Chemical Society*, 2007, **129**, 6453-6460.
80. G. Liu, T. B. Liu, S. S. Mal and U. Kortz, *Journal of the American Chemical Society*, 2006, **128**, 10103-10110.
81. T. B. Liu, M. L. K. Langston, D. Li, J. M. Pigga, C. Pichon, A. M. Todea and A. Muller, *Science*, 2011, **331**, 1590-1592.
82. P. C. Yin, D. Li and T. B. Liu, *Chemical Society Reviews*, 2012, **41**, 7368-7383.
83. R. A. Peterson, E. C. Buck, J. Chun, R. C. Daniel, D. L. Herting, E. S. Ilton, G. J. Lumetta and S. B. Clark, *Environmental Science and Technology*, 2018, **52**, 381-396.

84. E. Tiferet, A. Gil, C. Bo, T. Y. Shvareva, M. Nyman and A. Navrotsky, *Chemistry-a European Journal*, 2014, **20**, 3646-3651.
85. C. Falaise, S. M. Hickam, P. C. Burns and M. Nyman, *Chemical Communications*, 2017, **53**, 9550-9553.
86. F. Blanchard, M. Ellart, M. Rivenet, N. Vigier, I. Hablot, B. Morel, S. Grandjean and F. Abraham, *Crystal Growth & Design*, 2016, **16**, 200-209.
87. F. Blanchard, M. Ellart, M. Rivenet, N. Vigier, I. Hablot, B. Morel, S. Grandjean and F. Abraham, *Chemical Communications*, 2016, **52**, 3947-3950.
88. G. A. Senchyk, E. M. Wylie, S. Prizio, J. E. S. Szymanowski, G. E. Sigmon and P. C. Burns, *Chemical Communications*, 2015, **51**, 10134-10137.
89. N. Belai, M. Frisch, E. S. Ilton, B. Ravel and C. L. Cahill, *Inorganic Chemistry*, 2008, **47**, 10135-10140.
90. L. Chatelain, S. White, R. Scopelliti and M. Mazzanti, *Angewandte Chemie-International Edition*, 2016, **55**, 14325-14329.
91. C. Falaise, C. Volkringer, C. Hennig and T. Loiseau, *Chemistry-a European Journal*, 2015, **21**, 16654-16664.
92. C. Falaise, C. Volkringer, J. F. Vigier, A. Beaurain, P. Roussel, P. Rabu and T. Loiseau, *Journal of the American Chemical Society*, 2013, **135**, 15678-15681.

Table of Contents

Uranyl peroxide cages are an extensive family of topologically varied self-assembling nanoscale clusters with fascinating properties and applications.